European Journal of Cancer 171 (2022) 85–95

Available online at www.sciencedirect.com

ScienceDirect

journal homepage: www.ejcancer.com

Original Research

Copy number alterations in stage I epithelial ovarian cancer highlight three genomic patterns associated with prognosis

Chiara Pesenti [a,1], Luca Beltrame [b,1], Angelo Velle [c], Robert Fruscio [d], Marta Jaconi [e], Fulvio Borella [f], Fulvia Milena Cribiù [g], Enrica Calura [c], Lara Veronica Venturini [a], Deborah Lenoci [a], Federico Agostinis [c], Dionyssios Katsaros [h], Nicolò Panini [a], Tommaso Bianchi [d], Fabio Landoni [d], Monica Miozzo [i,j], Maurizio D'Incalci [k,l,*], James D. Brenton [m], Chiara Romualdi [c,2], Sergio Marchini [b,2]

[a] *Department of Oncology, Istituto di Ricerche Farmacologiche Mario Negri IRCCS, Milano, Italy*
[b] *IRCCS Humanitas Research Hospital, Rozzano, Italy*
[c] *Department of Biology, University of Padova, Padova, Italy*
[d] *Department of Obstetrics and Gynaecology, Università Degli Studi Milano-Bicocca, San Gerardo Hospital, Monza, Italy*
[e] *Department of Pathology, Università Degli Studi Milano-Bicocca, San Gerardo Hospital, Monza, Italy*
[f] *Gynecology and Obstetrics 1, Department of Surgical Sciences, San Anna Hospital, University of Torino, Torino, Italy*
[g] *Division of Pathology, Fondazione IRCCS Ca' Granda Ospedale Maggiore Policlinico, Milano, Italy*
[h] *AOU City of Health, Dept of Surgical Sciences, Gynecology, St Anna Hospital and University of Torino, Torino, Italy*
[i] *Department of Health Sciences, Medical Genetics, Università Degli Studi di Milano, Milano, Italy*
[j] *Research Laboratories Coordination Unit, Fondazione IRCCS Ca' Granda Ospedale Maggiore Policlinico, Milano, Italy*
[k] *Laboratory of Cancer Pharmacology, IRCCS Humanitas Research Hospital, Rozzano, Italy*
[l] *Department of Biomedical Sciences, Humanitas University, Pieve Emanuele, Italy*
[m] *Cancer Research UK Cambridge Research Institute, University of Cambridge, Cambridge, UK*

Received 3 February 2022; received in revised form 13 April 2022; accepted 3 May 2022
Available online 14 June 2022

KEYWORDS
Stage I EOC;
Somatic copy number alteration;

Abstract ***Background:*** Stage I epithelial ovarian cancer (EOC) encompasses five histologically different subtypes of tumors confined to the ovaries with a generally favorable prognosis. Despite the intrinsic heterogeneity, all stage I EOCs are treated with complete resection and adjuvant therapy in most of the cases. Owing to the lack of robust prognostic markers, this

* *Corresponding author*: Prof. Maurizio D'Incalci, Humanitas University, Department of Biomedical Sciences, Via Rita Levi Montalcini 4, 20072 Pieve Emanuele (MI), Italy.
E-mail address: maurizio.dincalci@hunimed.eu (M. D'Incalci).
[1] CP and LB contributed equally to this work. [2] CR and SM are co last authors.

https://doi.org/10.1016/j.ejca.2022.05.005

Prognosis

often leads to overtreatment. Therefore, a better molecular characterization of stage I EOCs could improve the assessment of the risk of relapse and the refinement of optimal treatment options.

Materials and methods: 205 stage I EOCs tumor biopsies with a median follow-up of eight years were gathered from two independent Italian tumor tissue collections, and the genome distribution of somatic copy number alterations (SCNAs) was investigated by shallow whole genome sequencing (sWGS) approach.

Results: Despite the variability in SCNAs distribution both across and within the histotypes, we were able to define three common genomic instability patterns, namely stable, unstable, and highly unstable. These patterns were based on the percentage of the genome affected by SCNAs and on their length. The genomic instability pattern was strongly predictive of patients' prognosis also with multivariate models including currently used clinico-pathological variables.

Conclusions: The results obtained in this study support the idea that novel molecular markers, in this case genomic instability patterns, can anticipate the behavior of stage I EOC regardless of tumor subtype and provide valuable prognostic information. Thus, it might be propitious to extend the study of these genomic instability patterns to improve rational management of this disease.

1. Introduction

The prognosis of patients diagnosed with epithelial ovarian cancer (EOC) confined to one or both ovaries (International Federation of Gynecology and Obstetrics, FIGO, stage I) is better than the prognosis of patients with disease widespread in the abdominal cavity (FIGO stage III/IV) [1,2]. According to the criteria defined by the "ICON1/ACTION" trial, all stage I EOC patients are treated with staging procedure, while only for a small subset of cases adjuvant platinum-based chemotherapy (CT) can be withheld, according to tumor grade and FIGO sub-stage [3]. These clinical/histological parameters are imperfect proxy of the risk of patients to relapse, and there is an urgent need to identify novel molecular-based classifiers to improve our ability to predict at the diagnosis the risk of patient relapse and identify those cases that, as a low risk to relapse, should be treated with surgery alone avoiding exposure to toxic effects of CT. The infrequent diagnosis of stage I EOC and the presence of at least five different histological subtypes (high-grade serous HGSOC, low-grade serous LGSOC, mucinous MOC, clear cell OCCC, and endometrioid EC) have limited till now translational studies aimed to answer this issue.

On a unique and retrospective cohort of more than 200 snap-frozen stage I EOC, our group identified integrated transcriptional signatures with a better prognostic predictivity than conventional clinico-pathological classifiers [4–6].

However, since gene expression classifiers are usually less feasible in clinical practice than genomic markers, we decided to assess the genomic landscape of stage I EOC subtypes to gain more insights into the molecular features of the disease and define novel potential predictive markers. In the present study, low pass whole genome sequencing (*alias* shallow whole genome sequencing, sWGS), approach was exploited to uncover the somatic copy number alterations (SCNAs) profile across the genome of 205 stage I tumor biopsies.

2. Materials and methods

2.1. Study cohort

A retrospective cohort of 205 tumor biopsies collected between 1989 and 2018 was selected from 225 stage I EOC tumor biopsies stored in Pandora tumor tissue collection at Istituto di Ricerche Farmacologiche Mario Negri, IRCCS (Milano, Italy) (Supplementary Fig. S1). Details are reported in the Supplementary Methods section 1 and Supplementary Results sections 1 and 2. Briefly, cases were gathered from two independent Italian clinical centers: San Gerardo Hospital (Monza, Italy) n = 172 (from now onward as cohort A) and Città della Salute (Torino, Italy) n = 53 (from now onward as cohort B), and recently revised by a second pathologist following the current guidelines of the World Health Organization for EOC [7]. The study was performed following the Declaration of Helsinki and the scientific ethical committee "Brianza" approved the collection and usage of tumor, blood, and plasma samples (N° 1065, on November 10th, 2015, emended on February 22nd, 2018). Written informed consent was obtained from all patients enrolled in the study.

2.2. Study design and methods

KAPA HyperPrep Kit (Roche, Basel, Switzerland) was exploited to perform sWGS, and experiments were run according to the manufacturer's instructions. In those

cases where tumor content cannot be evaluated by the pathologist, the Absolute Copy Estimator (ACE) tool [8] was used to infer the tumor purity and ploidy of each sample based on the results of single nucleotide variants (SNVs) calls obtained from an in house designed panel of 139 coding genes (Table S2). Absolute SCNAs profiles within each histotype were analyzed by the Genomic Identification of Significant Targets in Cancer algorithm (GISTIC) [9]. The copy number burden (CNB), the median SCNA length, and the number of SCNA in each tumor biopsy were determined and exploited to define the genome instability patterns. The potential prognostic role of these SCNAs patterns was investigated through univariate and multivariate analyses in combination with current prognostic variables considered in clinical practice. Details are available in the Supplementary Methods section.

2.3. Data availability

Sequence data have been submitted to European Genome-Phenome Archive (EGA; ID EGAS00001004961) and are available under controlled access.

3. Results

3.1. sWGS analysis reveals distinct SCNA distributions across the stage I EOC histotypes

The aim of our work was to define the genomic fingerprints which could be relevant for the prognosis of stage I EOC. To this end, we applied a low-resolution genome sequencing approach (*i.e.*, sWGS, 0.5X coverage) to a unique retrospective and multicentric cohort of 205 tumor biopsies originally selected from a tumor tissue collection of 225 stage I EOC patients, encompassing the five major histological subtypes (HGSOC, LGSOC, EC, OCCC, and MOC) with a mean follow-up of eight years (Fig. S1, Supplementary Results section 1). The demographic and clinical features reported in Table 1 show that the study cohort is histologically distributed and, as previously published [4–6], representative of the clinical situation (Supplementary Results section 2).

For each histological subtypes, we initially analyzed the distribution of SCNAs pattern and determined those SCNAs that were recurrent in each sample population. As the SCNA estimation is largely dependent on the

Table 1
Summary of the patients' clinicopathological features.

Clinical annotations	Number of patients	% of patients	Number of patients with FU	Median FU [IQR 1–3]
Histology and grade				
Mucinous			38	11.2y [7.2y-14.3y]
G1	26	13		
G2	10	5		
G3	1	0.5		
n.d	1	0.5		
Clear cells	29	14	28	5.7y [2.5y-14.3y]
Endometrioid			79	10.1y [6.6y-14.7y]
G1	14	7		
G2	38	18		
G3	28	14		
Low-grade serous	9	9	19	14.6y [10.3y-17.2y]
High-grade serous	39	19	39	7.3y [5.2y-15.7y]
FIGO substages				
A	68	33		
B	17	8		
C	116	57		
n.d	4	2		
Median age at diagnosis [min–max];	54.9y [16.5y – 89.3y]			
Chemotherapy				
Yes	148	72		
No	51	25		
n.d	6	3		
Relapse				
Yes	43	21		
No	145	71		
n.d	17	8		
PFS [IQR 1–3]	8.7y [4.8y –14.4y]			
OS [IQR 1–3]	10.1y [6y –15.5y]			
Total number of patients	205			

Note: G, grade; y, years; FU, Follow-up; PFS, progression-free survival; OS, overall survival; IQR, interquartile range.

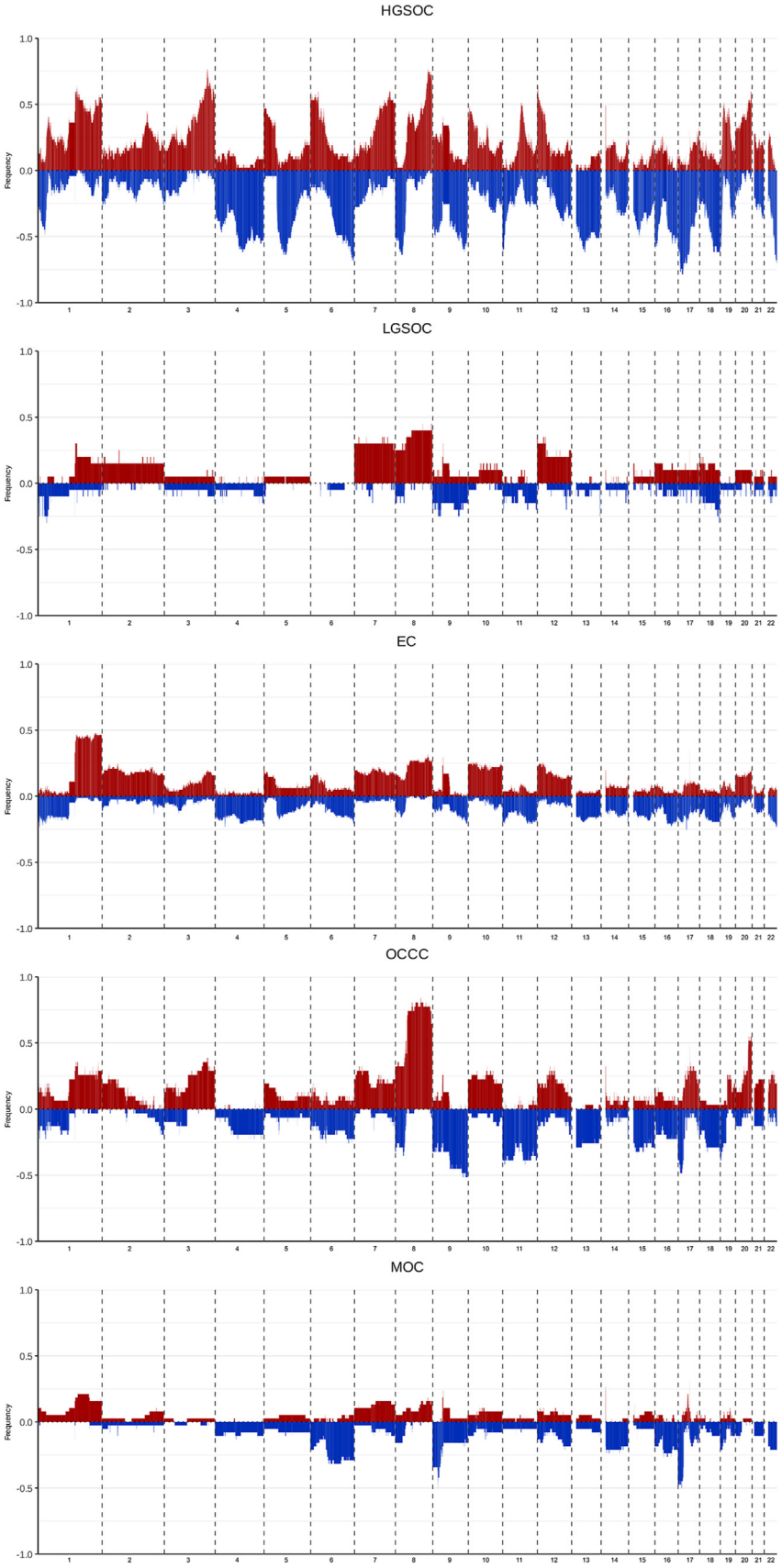

Fig. 1. **Distribution of SCNAs across the different histotypes**. Frequency plots distribution of SCNAs with at least one copy-number change (either gain or loss) from 205 tumor biopsies withdrawn from patients with the diagnosis of stage I EOC. Plots are presented according to the different histological subtypes. The 22 autosomal chromosomes are arranged horizontally along the x-axis, from largest (on left) to

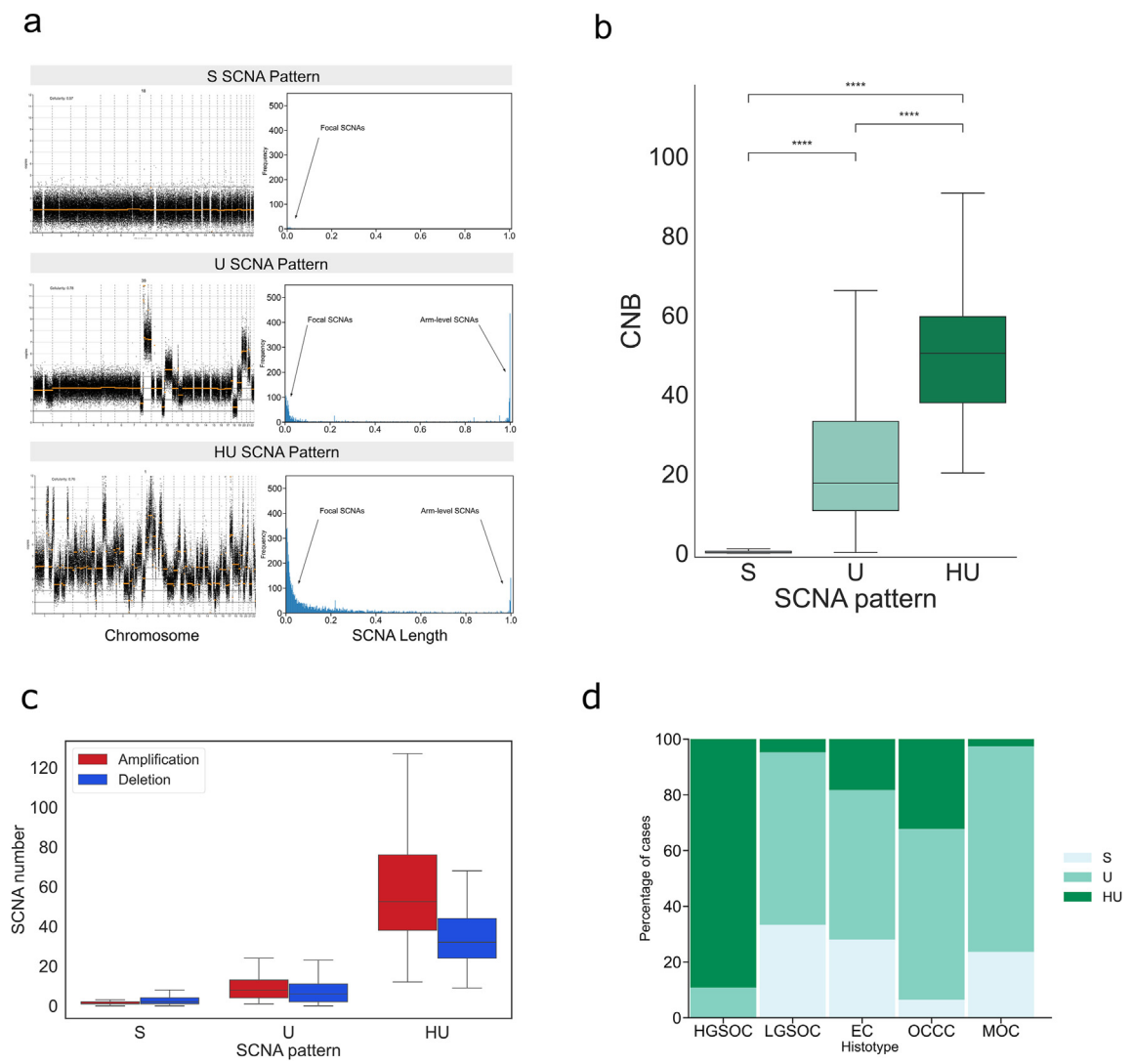

Fig. 2. **(a) SCNA patterns identified in stage I EOCs.** The left-hand panel reports log2 ratios (y-axis) for each 30kbp bin (black points) across the genome (x-axis, from chromosome 1 to chromosome 22) for the three representative cases of stable (S), unstable (U), and highly unstable (HU) SCNA pattern (cases n. 18, 39, and 1, respectively). The right-hand panels show the frequency (y-axis) of the length of DNA regions affected by SCNAs normalized per chromosome arm (ranging from 0, indicating focal SCNAs, to 1, entire chromosomal arm) for each SCNA pattern. **(b) Box plots of CNB distribution for each SCNA pattern.** The plot depicts the distribution of CNB, according to the S, U, and HU patterns. Boxes indicate the data range between the 25th and 75th percentile; the black line indicates the median value, and the bottom and top whiskers refer to the 5th and 95th percentile, respectively. ****, Mann–Whitney $p < 0.0001$. **(c) Number of SCNAs in each SCNA pattern.** The plots depict the number of amplification (red boxes) and deletions (blue boxes) according to the S, U, and HU patterns. Boxes indicate the data range between the 25th and 75th percentile; the black line indicates the median value, and the bottom and top whiskers refer to the 5th and 95th percentile, respectively. **(d) Distribution of S, U, and HU patterns according to the different histological subtypes.** The percentage of S, U, and HU tumor biopsies is represented for each of the five main histological subtypes of stage I EOC analyzed. Note: OCCC, clear cells. EC, endometrioid. MOC, mucinous. HGSOC, high-grade serous ovarian cancer. LGSOC, low-grade serous ovarian cancer.

tumor purity, we used the ACE algorithm [8] to accurately infer tumor purity and ploidy of each sample and then adjust the sWGS copy number profile accordingly (Supplementary Results section 3). GISTIC analysis [9] revealed a relatively different pattern of amplifications/deletions between HGSOC and the other histotypes

smallest, with "p" arms to the left. At each genomic location, the percentage of tumor biopsies with an aberration is shown on the y-axis. Only alterations with an absolute value of log2 ratio greater than 0.3 are reported. Red indicates recurrent copy number gain; blue indicates recurrent copy number loss. Note: HGSOC, high-grade serous ovarian cancer. LGSOC, low-grade serous ovarian cancer. EC, endometrioid. OCCC, clear cells. MOC, mucinous.

(Fig. 1). Globally, HGSOC cases were characterized by a high degree of genomic instability with almost all chromosomes harboring regions in gain or loss with variable sizes, ranging from 340 kbp to 76 Mbp. Differently, LGSOC, EC, OCCC, and MOC cases were characterized by a lower frequency of regions affected by SCNAs, mostly involving entire chromosome arms. GISTIC analysis defined three different types of SCNAs: (*i*) arm-level events, involving the entire chromosome arm (Table S5); (*ii*) focal SCNAs events, spanning less than 25% of the chromosome arm (Table S6); (*iii*) broad events, spanning more than 25% of the chromosome arm but less than its entirety (Table S6). Focusing on recurrent genomic alterations, HGSOC cases showed the highest degree of genomic instability and were characterized by many recurrent focal SCNAs in all chromosomes. In agreement with data previously published for stage III/IV HGSOC [10,11], the main recurrent focal amplification was on cytoband 8q24.21 on which the main oncogene is *MYC* (82% of cases, Table S6). Among the recurrent arm-level SCNAs, we identified a frequent deletion of the short arm of chromosome 17 (namely, 17p), where the *TP53* gene is located (72% of cases, Table S5), while among the recurrent broad events, we found a 6.6 Mb long deletion on cytoband 19p13.3, encompassing the *STK11* gene (62% of cases, Table S6); the 49.53 Mbp long deletion on cytoband 18q23, where the chromosomal instability suppressor gene *ZNF516* is located (62% of cases, Table S6) [12]; and a 31.35 Mbp deletion on cytoband 13q14.11 encompassing the *RB1* gene (60% of cases, Table S6). Focusing on the other histotypes, some recurrent SCNAs were observed in the OCCC subtype, while they were almost absent in LGSOC, EC, and MOC samples (Tables S5 and S6). The complete list of genes mapped in GISTIC peaks is reported in Table S7. Overall, these data depict a heterogeneous and complex landscape of SCNAs, both across the five histotypes and within the same histotype.

3.2. Three distinct macro-SCNA patterns indicate different degrees of genomic instability

Based on both the amount of the genome involved in SCNAs (i.e., CNB) and the size of SCNAs, three different genomic instability patterns could be clearly identified: stable (S), unstable (U), and highly unstable (HU). A representative case for each profile is reported in Fig. 2a. The S pattern (Fig. 2a, upper panel) had a median CNB of 0.13% (IQR 0.03–0.4%, Fig. 2b) and was characterized by a macroscopically stable genome with the absence of any relevant SCNA at either focal or arm-level. HE-staining and flow cytometry data, to exclude that the S profile was due to tumor purity or sample artifacts, we performed additional analysis by flow cytometry and Hematoxilin and eosin (H&E) staining on both snap frozen or matched formalin fixed, paraffin embedded (FFPE) tissue samples (Supplementary Results, sections 6 and 7). The U pattern (Fig. 2a, middle panel) had a median CNB of 17.65% (IQR 10.72–33.2%, Fig. 2b) and included cases that exhibited mainly large arm-level copy number rearrangements with a median of 14 SCNAs per sample (Fig. 2c). The HU cases (Fig. 2a, lower panel) had a median CNB of 50.38% (IQR 37.9–59.61%, Fig. 2b) and were characterized by many SCNAs (median 88 events, IQR 68–120, Fig. 2c), at both focal, broad, and arm-level. Figure 2d shows the distribution of SCNA patterns across each histotype. Approximately half of stage I EOC cases belonged to the U pattern (n = 104, 51%), which characterized the majority of LGSOC (63%), EC (53%), OCCC (59%), and MOC (74%) cases. A total of 34 out of 39 HGSOCs cases (87%) had a HU pattern, with the remaining five cases having U pattern. The high level of genomic instability in the HGSOC cases, reflected by the great prevalence of HU profile, also resulted in a significantly higher CNB compared to other histotypes (median CNB 51.5%, Mann–Whitney test $p < 0.001$; as shown in Fig. S4). The HU pattern encompassed also about 19% and 35% of EC and OCCC cases, respectively, while only one MOC (2.6%) and one LGSOC (5%) belonged to this category. The S pattern represented approximately 30% of LGSOC and EC tumors and 24% of MOC. Only two OCCC (7%) samples had an S pattern (Fig. 2d). Noteworthy, in a small subset of stage I cases with matched samples from both bilateral and relapsed biopsies, we observed that the identified SCNA pattern is shared by contralateral ovarian biopsy and its matched metachronous lesion after CT (Tables S9 and S10).

Finally, we questioned whether observed patterns of genomic instability were unique to stage I or could also be detected in stage III/IV tumor biopsies. Results from preliminary analysis on a cohort of 37 stage II-IV EOCs biopsies (Table S11) recapitulate the profiles obtained in stage I EOCs, with the HGSOCs characterized mainly by HU pattern and an heterogeneous distribution of the three profiles across the other histological subtypes (Figs. S5 and S6, and Table S12). As HGSOC is the most frequent subtypes observed in stage III/IV, we reasoned to validate this finding in two independent external datasets of HGSOC: (i) TCGA, which is the benchmark of HGSOC [13] and (ii) an in-house dataset of HGSOC cases from which ovarian tumor biopsies and matched synchronous lesions, naive to CT, were analyzed by sWGS approach [11]. This dataset was used to address the issue of spatial heterogeneity in stage III/IV HGSOC. Figure S7 confirmed that 96,1% of TCGA stage III/IV HGSOC cases harbor an the HU profile. This finding was further confirmed in the second independent dataset: 87.5% of cases (28 out of 32) were classified as HU

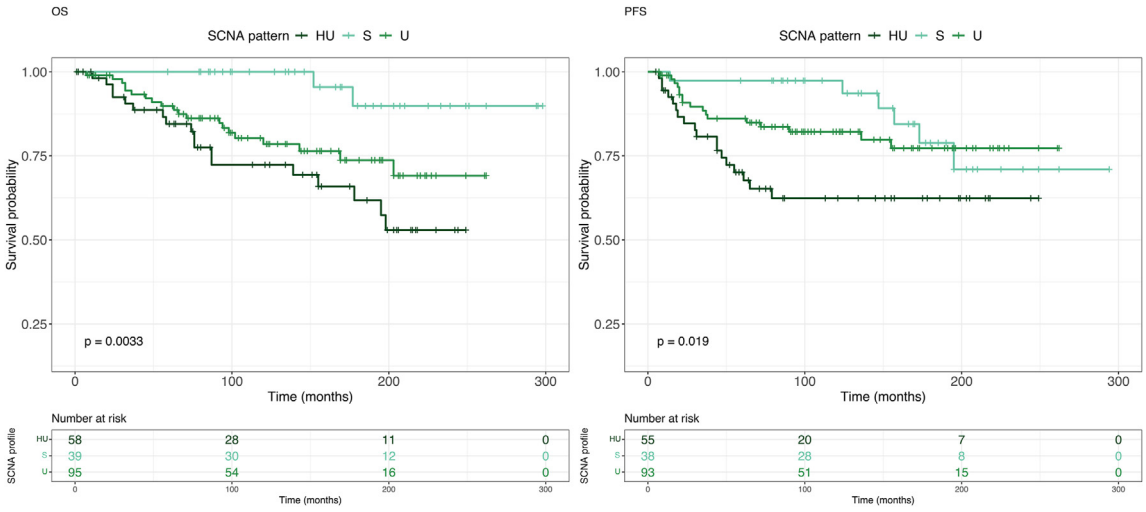

Fig. 3. **Kaplan–Meier curves show survival in patients belonging to the HU, U, and S groups.** OS (panel on the left) and PFS (panel on the right) survival analyses among the three groups HU (dark green), U (green), and S (light green) on the entire samples cohort. Univariate log-rank test p-values are reported within each plot along with the risk table.

while 12.5% (4 out of 32) were classified as U, while no case was found with S profile (Table S13). To note, for all the cases, the profile identified in the ovary (referred as "A" biopsy) was the same of the matched synchronous lesions (referred as "B", "C", "D", *etc.*; Table S13). These preliminary data suggest that the identified SCNA profile is an early molecular feature of the tumor rather than a late passenger event.

As a corollary, to make sample classification automatic, we used a classification tree algorithm to precisely identify SCNA variables cutoffs that maximized correct classification. As depicted in Fig. S8, we trained the algorithms on the 130 cases for which the instability pattern was clearly ascribable as S (n = 20), U (n = 70), and HU (n = 40) obtaining, with a cross-validation strategy, a 11% error rate. The model was then applied to predict the SCNA pattern of the remaining 75 samples obtaining an 8% error rate (Supplementary Methods, Supplementary Results section 10).

3.3. Association of SCNA genomic profiles with ISC expression signature

On the same samples used in this study, our group recently identified a transcriptional signature called integrated signature classifier (ISC), composed of 16

Table 2
Multivariate Cox proportional hazard models (OS and PFS) comparing SCNA patterns adjusted for grade, FIGO 2, chemotherapy (CT), *TP53* mutation status, and age. Hazard Ratio (HR) with confidence interval at 95% of confidence (CI 95%) and p-value are reported. Highly ($p < 0.05$) and moderately significant ($p < 0.1$) variables are marked in bold.

	PFS			OS		
	HR	CI (95%)	P-value	HR	CI (95%)	P-value
SCNA profile						
Stable (reference)	–	–	–	–	–	–
Unstable	1.48	0.57–3.82	0.417	5.10	1.16–22.36	**0.031**
Highly unstable	1.54	0.48–4.96	0.470	4.39	0.78–24.70	**0.093**
Grade						
Low (reference)	–	–	–	–	–	–
High	1.78	0.83–3.80	0.138	1.67	0.76–3.68	0.204
FIGO 2						
a (reference)	–	–	–	–	–	–
B	0.47	0.10–2.26	0.349	2.97	0.80–10.94	0.103
C	1.34	0.62–2.93	0.460	3.06	1.26–7.42	**0.013**
TP53						
WT (reference)	–	–	–	–	–	–
Yes	1.36	0.59–3.13	0.471	1.07	0.45–2.55	0.883
CT						
No (reference)	–	–	–	–	–	–
Yes	5.52	1.20–25.43	**0.028**	0.61	0.25–1.48	0.274
Age						
	1.00	0.98–1.03	0.863	1.05	1.02–1.08	**0.001**

miRNAs and ten coding genes, with high and significant prognostic properties and with higher classification performance than conventional clinical classifiers [4]. Using ROC analyses, samples were divided into two groups for both overall survival (OS) and progression-free survival (PFS), namely high and low-risk groups.

Here, we explored if the SCNAs genomic profiles were correlated with ISC classes. Interestingly, we found that cases with an S genomic instability pattern were almost always (with the exception of one case for OS and two cases for PFS) classified as low risk by the ISC, with a low risk of relapse and with a better prog nosis (chi-squared test p-value = 0.04 for OS and p-value = 0.11 for PFS).

3.4. Association of SCNA genomic profiles with clinical variables

Finally, the S, U, and HU profiles were associated with clinical variables for prognostic purposes. Using univariate models, we found that the three SCNA patterns were significantly associated with survival in terms of both PFS (p = 0.019) and OS (p = 0.003) (Fig. 3). Although in the PFS survival curve a decrease in survival can be observed after ten years of follow-up in the S profile, the uncertainty of the last part of the curve is very large, and the difference between S and U profiles is not significant. Association with OS was significant even in multivariate models when FIGO substage, grading, age, CT treatment, and *TP53* status were included as covariates (Table 2). Patients with U and HU patterns had significantly worse OS compared to those in the S group (HU vs S HR = 4.39, CI95% = 0.78−24.70, p = 0.09; U vs S HR = 5.1, CI95% = 1.16−22.36, p = 0.03), while such differences were not observed between patients in HU and U (HR = 0.90, CI95% = 0.43−1.88, p = 0.78). As stage I is characterized by different morphology, multivariate analysis integrating the SCNA patterns with histotypes, grade, FIGO 2, and age confirmed a moderate association of U and HU profiles to a worse OS (Table S14). These results strengthen the prognostic role of the SCNA pattern, independently of tumor histotype.

Since HGSOC was prevalent in the HU pattern (56%) and HGSOCs and OCCCs are usually characterized by a worse prognosis, we assessed the effect of these histological subtypes on survival. The univariate model shows that OS rates differ between SCNA groups even when the two histotypes with the worst prognosis in stage I EOC, namely OCCCs and HGSOC, were excluded (Table S15).

Lastly, we checked whether the significant survival trends among cases with the same SCNA pattern would be confirmed when considering the two sample cohorts separately. Supplementary Tables S16 and S17 show the clinico-pathological characteristics divided by clinical centers, while Fig. S9 shows the survival plots. Except for PFS in cohort A, U, and HU showed a significantly worse prognosis than S in both patient groups.

In conclusion, the unique SCNA landscape of stage I tumor biopsies at diagnosis can help deciphering the risk of relapse independently from currently used clinical/pathological parameters.

4. Discussion

In the present study, genomic landscape analysis of a unique cohort of 205 stage I EOCs allowed us to extend the current knowledge of the complex and heterogeneous biology behind the conventional histological classification of stage I EOC and to find promising correlations with clinical parameters. Briefly, data can be summarized as follows:

1. sWGS profiles provide a quantification of tumor heterogeneity among patients and histotypes.
2. The genomic data provides a refinement of current morphological classification.
3. The genome classifier sounds to be useful in predicting the prognosis of stage I EOC.

Over the last years, genomic signatures based on SCNA data are growing in importance for predictive purposes [14], but their clinical utility has been limited by the amount and complexity of data generated. In this study, we demonstrated that low-pass whole genome sequencing is a valuable tool to shed new lights on the diagnosis and prognosis of stage I EOC. sWGS data revealed a heterogeneous SCNAs distribution across the five different histological subtypes. The analysis identified three distinct patterns of genomic instability, namely S, U, and HU, defined by the levels and the extent of copy number events in the genome. These patterns were differently distributed among the five histotypes, with a prevalence of U patterns among all the histotypes but HGSOC. Particularly, HGSOC were characterized by a prevalence of the HU pattern, in line with the notion that even at early precursor lesions, this histotype has the highest degree of genomic instability [15,16], with many recurrent focal events affecting both relevant onco-suppressors and oncogenes. Particularly, the vast majority of HGSOCs harbored a chromosome 17p deletion, a well-recognized SCNA that causes the complete inactivation of *TP53* gene, the early precursor event of this histotype [17]. Another recurrent SCNA that characterize the HGSOC subtype is the deletion of cytoband 13q14.11 where the *RB1* tumor suppressor gene is mapped, which has already been reported to occur in the early steps of tumor progression and correlate with different clinical outcomes and therapy response [18]. In parallel, the most recurrent focal amplification in HGSOCs affected the *MYC* oncogene, which was already reported in FIGO stages I and II to be correlated with a worse prognosis [19]. Other genes

affected by recurrent SCNAs in HGSOCs are *STK11* (or *LKB1*) and *ZNF516*, both included into two regions where broad deletions occurred in about 60% of cases, chromosomes 19p13.3 and 18q23, respectively. *STK11* is the causative gene of the Peutz-Jeghers syndrome, one of the germline syndromes associated with increased susceptibility to different tumors, among which breast and ovarian tumors [20]. The loss of the LKB1 activity has been reported to be an early tumorigenic event favoring the development of HGSOC from ovarian surface epithelial cells in murine models along with the deletion of *PTEN* [21] and to participate in the upregulation of the NF-κB pathway in HGSOC cells models [22]. On the contrary, ZNF516 is a less known Zinc Finger protein involved in transcription regulation, but its cellular functions are not completely described; yet, it has been involved in replication stresses and particularly its loss was associated with increases chromosome instability along with other potential tumor suppressor genes located on the same chromosome arm, 18q [12], and further studies will be necessary to clarify the role of this gene in genomic instability.

As clonal pathogenic variants in the *TP53* gene are considered the founder hallmark of HGSOC [17], we reasoned whether the HU profile could be explained by *TP53* alterations. Although we found a strong association between HU profile and *TP53* mutations, we observed a small fraction of *TP53* mutated cases with a U profile and some HU samples without *TP53* mutation. Thus, our results are not conclusive regarding the etiopathogenic role of *TP53* mutations in leading HU profile but suggest a more complex scenario that requires further studies to be properly addressed. Although very preliminary, the finding that on a small cohort of cases, the identified SCNA patterns are shared in matched bilateral biopsies, and in relapsed disease after platinum-based CT suggests that the S, U, and HU profiles could be drivers of genomic fingerprints of the disease. Analysis on two small retrospective cohorts of stage II/III/IV EOCs confirmed the same SCNA patterns. The S profile was observed in MOC and EC subtypes while HGSOCs were almost all HU, as further confirmed in TCGA data. Overall, these data suggest that genomic heterogeneity is a key factor underlying our inability to fit tumor behavior into a rigid histological classification and open the possibility of further stratification of tumor histotypes based on genomic patterns that are more indicative of different etiopathogenic processes. Regarding the analysis of stage III/IV samples, which differently from stage I cases, are characterized by multiple metastases, it is still to uncover if the genomic pattern of multiple synchronous lesions would be different in different anatomical sites of the same patient.

These three genomic patterns might, therefore, represent a tool to help divulge the behavior of each stage I EOC and its prognostic evolution. Intriguingly, we found that the presence of different patterns of genomic instability (HU and U) correlated with OS, even in a multivariate analysis with the currently used clinical parameters. A similar trend was observed even when HGSOC and OCCC were excluded from the analysis. The fact that this type of molecular analysis could be performed on formalin fixed and paraffin embedded tumor biopsies (which are routinely stored in hospitals) and that it requires a relatively straightforward nature of data evaluation, makes it clinically feasible and relatively inexpensive. In this perspective, we have developed an in-house algorithm that, once validated prospectively, would make the analysis reproducible and obviates the subjective interpretation.

Although our results uncover new molecular characteristics of early-stage EOCs, our work has some limitations that have to be mentioned. First, the size of the cohort precluded a separate survival analysis for each histotype to further confirm the prognostic role of the SCNAs patterns within each tumor subtype. Moreover, it also prevented a deeper investigation of molecular features and mechanisms associated with each SCNA pattern. However, given the rarity of stage I EOC, the cohort studied here is one of the largest ever analyzed. Further multi-center studies will be necessary to support the results described here. Second, our survival analysis was not run on an independent dataset to confirm our findings. Yet, to our knowledge, sufficiently detailed and large public sequencing datasets of stage I EOC are currently not available.

In conclusion, our results, similarly to the recent genomic based reclassification of endometrial cancer [23], open the possibility to develop a novel molecular taxonomy for stage I EOC that is important for not only understanding of tumor biology but also differences in clinical behaviors of EOC.

Funding

The “Alessandra Bono Foundation” supported young investigators fellowships and the genomic infrastructure of the Department of Oncology. CP was supported by Italian Association for Cancer Research fellowship (id. 24148). SM is supported by the Italian Association for Cancer Research (grant number IG19997). CR is supported by the Italian Association for Cancer Research (grant number IG21837). The “Nerina and Mario Mattioli” Foundation supported the activity of Pandora tumor tissue collection.

Author contribution

Chiara Pesenti: conceptualization, data curation, formal analysis, investigation, methodology, validation, writing - original draft, and writing - review & editing. Luca Beltrame: conceptualization, data curation, formal analysis, investigation, methodology, software,

visualization, writing - original draft, and writing - review & editing. Angelo Velle: data curation, formal analysis, methodology, software, visualization, writing - original draft, and writing - review & editing. Robert Fruscio: data curation, investigation, project administration, resources, and writing - review & editing. Marta Jaconi: data curation, resources, and writing - review & editing. Fulvio Borella: data curation, resources, and writing - review & editing. Fulvia Milena Cribiù: data curation, investigation, and writing - review & editing. Enrica Calura: formal analysis, methodology, software, and writing - review & editing. Lara Veronica Venturini: investigation. Deborah Lenoci: investigation. Federico Agostinis: methodology and software. Dionyssios Katsaros: data curation, investigation, and writing - review & editing. Nicolò Panini: investigation, methodology, and validation. Tommaso Bianchi: data curation, investigation, and resources. Fabio Landoni: conceptualization, funding acquisition, project administration, resources, supervision, and writing - review & editing. Monica Miozzo: conceptualization, funding acquisition, project administration, supervision, and writing - review & editing. Maurizio D'Incalci: conceptualization, funding acquisition, project administration, supervision, writing - original draft, and writing - review & editing. James D. Brenton: conceptualization, formal analysis, funding acquisition, methodology, supervision, writing - original draft, and writing - review & editing. Chiara Romualdi: conceptualization, data curation, formal analysis, funding acquisition, investigation, methodology, resources, software, supervision, visualization, writing - original draft, and writing - review & editing. Sergio Marchini: conceptualization, funding acquisition, supervision, writing - original draft, and writing - review & editing.

Conflict of interest statement

The authors declare that they have no known competing financial interests or personal relationships that could have appeared to influence the work reported in this paper.

Acknowledgments

We would like to thank all patients who participated. We are grateful to Professor Andreas Gescher (University of Leicester, Leicester, UK) for critical revision and editing of the manuscript. We thank the "Cloud4CARE" project for providing the computational resources for data analysis, and Sara Potente for additional support for the bioinformatics analysis.

Appendix A. Supplementary data

Supplementary data to this article can be found online at https://doi.org/10.1016/j.ejca.2022.05.005.

References

[1] Berek JS, Renz M, Kehoe S, et al. Cancer of the ovary, fallopian tube, and peritoneum: 2021 update. Int J Gynaecol Obstet 2021; 155(1):61–85.
[2] American Joint Committee on Cancer. Ovary, fallopian tube, and primary peritoneal carcinoma. In: AJCC cancer staging manual. 8th ed. New York, NY: Springer; 2017. p. 681–90.
[3] Collinson F, Qian W, Fossati R, Lissoni A, Williams C, Parmar M, et al. Optimal treatment of early-stage ovarian cancer. Ann Oncol 2014;25:1165–71. https://doi.org/10.1093/annonc/mdu116.
[4] Calura E, Paracchini L, Fruscio R, DiFeo A, Ravaggi A, Peronne J, et al. A prognostic regulatory pathway in stage I epithelial ovarian cancer: new hints for the poor prognosis assessment. Ann Oncol 2016;27:1511–9. https://doi.org/10.1093/annonc/mdw210.
[5] Calura E, Ciciani M, Sambugaro A, Paracchini L, Benvenuto G, Milite S, et al. Transcriptional characterization of stage I epithelial ovarian cancer: a multicentric study. Cells 2019;8. https://doi.org/10.3390/cells8121554.
[6] Martini P, Paracchini L, Caratti G, Mello-Grand M, Fruscio R, Beltrame L, et al. lncRNAs as novel indicators of patients' prognosis in stage I epithelial ovarian cancer: a retrospective and multicentric study. Clin Cancer Res : An Official Journal of the American Association for Cancer Research 2017;23:2356–66. https://doi.org/10.1158/1078-0432.CCR-16-1402.
[7] WHO Classification of Tumours Editorial Board. Female genital tumours: WHO classification of tumours. 5th ed., vol. 4. Lyon, France: IARC; 2020.
[8] Poell JB, et al. ACE: absolute copy number estimation from low-coverage whole- genome sequencing data. Bioinformatics 2019. https://doi.org/10.1093/bioinformatics/bty1055.
[9] Mermel CH, et al. GISTIC2.0 facilitates sensitive and confident localization of the targets of focal somatic copy-number alteration in human cancers. Genome Biol 2011. https://doi.org/10.1186/gb-2011-12-4-r41.
[10] Ballabio S, Craparotta I, Paracchini L, Mannarino L, Corso S, Pezzotta MG, et al. Multisite analysis of high-grade serous epithelial ovarian cancers identifies genomic regions of focal and recurrent copy number alteration in 3q26.2 and 8q24.3. Int J Cancer 2019;145:2670–81. https://doi.org/10.1002/ijc.32288.
[11] Paracchini L, Beltrame L, Grassi T, Inglesi A, Fruscio R, Landoni F, et al. Genome-wide copy-number alterations in circulating tumor DNA as a novel biomarker for patients with high-grade serous ovarian cancer. Clin Cancer Res 2021;27: 2549–59. https://doi.org/10.1158/1078-0432.CCR-20-3345.
[12] Burrell RA, McClelland SE, Endesfelder D, Groth P, Weller M-C, Shaikh N, et al. Replication stress links structural and numerical cancer chromosomal instability. Nature 2013;494:492–6. https://doi.org/10.1038/nature11935.
[13] Cancer Genome Atlas Research Network. Integrated genomic analyses of ovarian carcinoma. Nature 2011;474:609–15. https://doi.org/10.1038/nature10166.
[14] Severson TM, Peeters J, Majewski I, Michaut M, Bosma A, Schouten PC, et al. BRCA1-like signature in triple negative breast cancer: molecular and clinical characterization reveals subgroups with therapeutic potential. Molecular Oncology 2015;9:1528–38. https://doi.org/10.1016/j.molonc.2015.04.011.
[15] Labidi-Galy SI, Papp E, Hallberg D, Niknafs N, Adleff V, Noe M, et al. High grade serous ovarian carcinomas originate in the fallopian tube. Nat Commun 2017;8:1093. https://doi.org/10.1038/s41467-017-00962-1.
[16] Asaka S, Davis C, Lin S-F, Wang T-L, Heaphy CM, Shih I-M. Analysis of telomere lengths in p53 signatures and incidental serous tubal intraepithelial carcinomas without concurrent ovarian cancer. Am J Surg Pathol 2019;43:1083–91. https://doi.org/10.1097/PAS.0000000000001283.

[17] Chien J, Sicotte H, Fan J-B, Humphray S, Cunningham JM, Kalli KR, et al. TP53 mutations, tetraploidy and homologous recombination repair defects in early stage high-grade serous ovarian cancer. Nucleic Acids Res 2015;43:6945–58. https://doi.org/10.1093/nar/gkv111.

[18] Milea A, George SH, Matevski D, Jiang H, Madunic M, Berman HK, et al. Retinoblastoma pathway deregulatory mechanisms determine clinical outcome in high-grade serous ovarian carcinoma. Mod Pathol 2014;27:991–1001. https://doi.org/10.1038/modpathol.2013.218.

[19] Skírnisdóttir IA, Sorbe B, Lindborg K, Seidal T. Prognostic impact of p53, p27, and C-MYC on clinicopathological features and outcome in early-stage (FIGO I-ii) epithelial ovarian cancer. Int J Gynecol Cancer 2011;21. https://doi.org/10.1097/IGC.0b013e31820986e5.

[20] Piombino C, Cortesi L, Lambertini M, Punie K, Grandi G, Toss A. Secondary prevention in hereditary breast and/or ovarian cancer syndromes other than BRCA. Journal of Oncology 2020;2020:e6384190. https://doi.org/10.1155/2020/6384190.

[21] Tanwar PS, Mohapatra G, Chiang S, Engler DA, Zhang L, Kaneko-Tarui T, et al. Loss of LKB1 and PTEN tumor suppressor genes in the ovarian surface epithelium induces papillary serous ovarian cancer. Carcinogenesis 2014;35:546–53. https://doi.org/10.1093/carcin/bgt357.

[22] Buensuceso A, Fritz JL, Collins O, Valdés YR, Borrelli MJ, DiMattia GE, et al. Loss of LKB1-NUAK1 signalling enhances NF-κB activity in a spheroid model of high-grade serous ovarian cancer. Sci Rep 2022;12:3011. https://doi.org/10.1038/s41598-022-06796-2.

[23] Kommoss S, et al. Final validation of the ProMisE molecular classifier for endometrial carcinoma in a large population-based case series. Ann Oncol 2018;29:1180–8.